algorithms

IMPACT FACTOR 2.1

CITESCORE 4.5

Article

Editor's Choice

Transmit and Receive Diversity in MIMO Quantum Communication for High-Fidelity Video Transmission

Udara Jayasinghe, Prabhath Samarathunga, Thanuj Fernando and Anil Fernando

MDPI

https://doi.org/10.3390/a18070436

algorithms

MDPI

Article

Transmit and Receive Diversity in MIMO Quantum Communication for High-Fidelity Video Transmission

Udara Jayasinghe, Prabhath Samarathunga, Thanuj Fernando and Anil Fernando *

Department of Computer and Information Sciences, University of Strathclyde, Glasgow G1 1XQ, UK; udara.jayasinghe-mudalige@strath.ac.uk (U.J.); prabhath.samarathunga@strath.ac.uk (P.S.); thanuj.fernando.2023@uni.strath.ac.uk (T.F.)

* Correspondence: anil.fernando@strath.ac.uk

Abstract

Reliable transmission of high-quality video over wireless channels is challenged by fading and noise, which degrade visual quality and disrupt temporal continuity. To address these issues, this paper proposes a quantum communication framework that integrates quantum superposition with multi-input multi-output (MIMO) spatial diversity techniques to enhance robustness and efficiency in dynamic video transmission. The proposed method converts compressed videos into classical bitstreams, which are then channel-encoded and quantum-encoded into qubit superposition states. These states are transmitted over a 2×2 MIMO system employing varied diversity schemes to mitigate the effects of multipath fading and noise. At the receiver, a quantum decoder reconstructs the classical information, followed by channel decoding to retrieve the video data, and the source decoder reconstructs the final video. Simulation results demonstrate that the quantum MIMO system significantly outperforms equivalent-bandwidth classical MIMO frameworks across diverse signal-to-noise ratio (SNR) conditions, achieving a peak signal-to-noise ratio (PSNR) up to 39.12 dB, structural similarity index (SSIM) up to 0.9471, and video multi-method assessment fusion (VMAF) up to 92.47, with improved error resilience across various group of picture (GOP) formats, highlighting the potential of quantum MIMO communication for enhancing the reliability and quality of video delivery in next-generation wireless networks.

Keywords: MIMO; quantum communication; quantum superposition; receive diversity; transmit diversity

Academic Editor: Frank Werner

Received: 24 June 2025
Revised: 8 July 2025
Accepted: 16 July 2025
Published: 16 July 2025

Citation: Jayasinghe, U.; Samarathunga, P.; Fernando, T.; Fernando, A. Transmit and Receive Diversity in MIMO Quantum Communication for High-Fidelity Video Transmission. *Algorithms* **2025**, *18*, 436. https://doi.org/10.3390/a18070436

1. Introduction

The ability to reliably deliver high-quality video content across diverse communication networks is a critical enabler of many modern digital applications, including telemedicine, remote learning, augmented [1] and virtual reality [2], autonomous driving, cloud gaming, and collaborative robotics. Unlike static image transmission, video communication requires not only high spatial resolution, but also temporal continuity to preserve motion fidelity and dynamic scene information. As users increasingly demand high definition (HD), ultra high definition (UHD) and immersive 360-degree video experiences [3], communication systems must meet stringent constraints on bandwidth, latency, and robustness against channel impairments. These challenges become even more severe in wireless environments, where time-varying fading, multipath propagation, and Doppler effects can cause significant signal degradation, packet loss, and fluctuations in link quality, all of which impact the reliability and quality of transmitted video.

To cope with the high bandwidth requirements of video, traditional transmission pipelines rely on source coding with advanced video compression standards such as H.264/AVC, H.265/HEVC, VP9, or AV1. These codecs achieve impressive compression efficiency by exploiting temporal redundancies across frames (through motion estimation and compensation) and spatial redundancies within frames. However, this compression strategy introduces significant vulnerability to transmission errors. A single corrupted bit, particularly in compressed bitstreams with inter-frame dependencies, can cause artifacts that propagate across multiple frames and degrade the perceived quality of the video. This problem becomes especially pronounced in time-varying and hostile channel conditions, where the combined effects of fading, interference, and noise make it challenging to maintain acceptable video quality and a smooth viewing experience.

To mitigate these effects, classical communication systems employ a variety of signal processing and coding strategies. Techniques such as adaptive modulation, forward error correction (FEC), automatic repeat request (ARQ), and multi-input multi-output (MIMO) spatial diversity have demonstrated success in improving the reliability and efficiency of video transmission in wireless environments. In particular, MIMO techniques [4,5] enhance robustness by exploiting multiple antennas at the transmitter and receiver to combat multipath fading and improve spectral efficiency. This MIMO transmission can be broadly categorized into four types: single-input single-output (SISO), which lacks spatial diversity; multi-input single-output (MISO), which employs transmit diversity; single-input multi-output (SIMO), which utilizes receive diversity; and multi-input multi-output (MIMO), which combines both transmit and receive diversity for enhanced performance. Although these diversity techniques have proven effective in enhancing data throughput and improving reliability, these classical methods encounter limitations in highly dynamic or bandwidth-constrained environments, where trade-offs between latency, complexity, and error resilience become more pronounced.

In response, quantum communication presents a new paradigm for data transmission, offering fundamentally different properties that can be harnessed for video delivery. Quantum superposition [6] enables qubits to encode multiple states simultaneously, thereby increasing the potential information capacity of the channel. Furthermore, quantum entanglement [7] provides correlations between qubits that classical systems cannot replicate, offering new mechanisms for coordinating and safeguarding information across a distributed system. When properly integrated, these quantum properties open up possibilities for improving throughput, enhancing noise resilience, and achieving higher reliability under adverse channel conditions. Despite the significant attention that quantum communication has received in the fields of cryptography and secure key distribution using quantum entanglement, the use of quantum superposition in media transmission, especially for dynamic video content, remains largely unexplored and untapped. In particular, the potential of quantum MIMO systems for dynamic video transmission has not been fully investigated. Although MIMO techniques, long established in classical wireless communications, improve reliability and data rates by exploiting spatial diversity through multiple transmit and receive paths, they also face several limitations, including increased hardware complexity, higher power consumption, challenges in accurate channel estimation, and reduced noise resilience. Extending MIMO principles into quantum communication could overcome these limitations and offer additional benefits by combining spatial diversity with quantum superposition. Specifically, this integration has the potential to enhance robustness against channel impairments such as fading and interference while increasing spectral efficiency.

Therefore, we propose a quantum MIMO system that combines quantum superposition with spatial diversity to enable reliable video transmission over channels subject to

severe fading and dynamic impairments. This work marks a pioneering effort in quantum MIMO-based video communication without prior research. To assess its effectiveness, we evaluate the system across multiple MIMO configurations, including transmit diversity (2×1 MISO), receive diversity (1×2 SIMO), and no diversity (1×1 SISO), demonstrating the benefits of quantum-assisted spatial diversity for next-generation video transmission systems.

In this proposed novel MIMO-based quantum-assisted video transmission framework, we integrate the following key components:

- Quantum superposition-based encoding, increasing resilience to noise, and enhancing throughput.
- Classical polar coding as an outer channel code, providing structured error correction for the quantum-encoded data stream.
- MIMO spatial diversity techniques (including 2×1 MISO, 1×2 SIMO, and 1×1 SISO configurations) for combating multipath fading in quantum communication channels.

A detailed simulation study is presented in which the proposed framework is evaluated under Rayleigh flat-fading channel conditions across a range of signal-to-noise ratio (SNR) levels. In the proposed method, the input videos are first source-encoded to obtain compressed representations, from which the classical bitstream is extracted. This bitstream is then channel-encoded using a polar code with a rate of $1/2$. The channel-encoded bitstreams are subsequently converted into quantum superposition states and transmitted through the aforementioned spatial diversity schemes over quantum channels. At the receiver, the received qubit superposition states are first quantum-decoded to recover the classical bitstreams. These are then channel-decoded and source-decoded to reconstruct the original video content. The system is evaluated using standard compressed video sequences, measuring quality through the peak signal-to-noise ratio (PSNR), structural similarity index (SSIM), and video multi-method assessment fusion (VMAF). For benchmarking purposes, we compare the performance of the quantum MIMO system against an equivalent classical MIMO system operating under identical bandwidth and diversity configurations.

The major contributions of this study are:

- The introduction of a quantum superposition-enhanced video transmission system that combines quantum principles with MIMO diversity to address the challenges of transmitting compressed video over fading channels.
- A comparative analysis that demonstrates the advantages of quantum-assisted transmission over classical approaches in terms of preserving video quality under adverse conditions.
- A flexible simulation-based framework adaptable for evaluating end-to-end quantum communication in video or multimedia transmission, providing an effective solution to fading in real-world communication scenarios.

The remainder of this paper is structured as follows. Section 2 reviews prior work on quantum communication for media transmission, classical MIMO diversity techniques, and existing quantum MIMO systems. Section 3 describes the proposed quantum MIMO transmission framework and describes the system model and simulation setup. Section 4 presents and analyzes the simulation results. Finally, Section 5 concludes the paper and discusses potential avenues for future research in quantum-enhanced video communication.

2. Related Works

Quantum communication is an emerging discipline at the intersection of quantum mechanics [8] and information science, which uses the unique phenomena of quantum physics to revolutionize the way data are transmitted and secured. Two fundamental principles form the cornerstone of this field: quantum entanglement [9] and quantum superposition [10]. Quantum entanglement refers to the remarkable phenomenon in which pairs or groups of particles become interconnected so that the state of one instantaneously influences the state of another, regardless of the distance separating them. This nonclassical correlation has been the foundation for groundbreaking applications such as quantum key distribution (QKD) [11–13], which offers theoretically unbreakable encryption methods by exploiting the properties of entangled particles to securely share cryptographic keys. Similarly, quantum teleportation utilizes entanglement to transfer the quantum state of a particle to another distant particle, effectively transmitting information without moving the physical particle itself [14,15]. Beyond secure key exchange, entanglement has been investigated for secure media transmission, including images and video, offering promising avenues to protect sensitive multimedia content [16–18].

On the other hand, quantum superposition gives quantum bits (qubits) the remarkable ability to exist in multiple states at the same time, unlike classical bits that can only represent a 0 or a 1 at any given moment. This unique property significantly increases the data capacity and parallelism that can be achieved in quantum communication systems. By encoding information into superposed qubits, it becomes possible to transmit multiple states of data simultaneously. This not only increases the potential throughput of the communication system, but can also enhance its resilience against noise, interference, and other channel impairments. Although some studies have explored the theoretical impact of superposition on communication complexity [19–21] and efficiency, and a few early applications have demonstrated its potential in basic image and video transmission using basic encoding and decoding techniques [22–24], the field is still in its early stages in terms of practical implementation. In particular, there is still a vast and largely untapped opportunity to combine quantum superposition with advanced quantum encoding techniques and robust error correction strategies. A practical, end-to-end quantum communication framework that leverages these capabilities is especially needed for demanding multimedia applications such as dynamic video transmission. Building such a system introduces unique challenges, including handling temporal dependencies between frames, supporting high data rates, and ensuring reliable reconstruction of the video stream despite the presence of channel noise and fading. Moreover, existing research has yet to fully investigate how quantum communication systems perform under realistic conditions where channel fading plays a critical role.

In practical wireless and optical communication scenarios, fading caused by multipath propagation, mobility, and atmospheric disturbances can severely degrade signal quality and reliability. To address these challenges, classical communication systems often utilize MIMO technology [25,26]. In MIMO, diversity reception techniques, such as time, frequency, and spatial diversity, are commonly employed to combat fading by leveraging multiple independent signal paths [27–29]. Over the years, researchers have developed various versions of MIMO systems and diversity schemes for a wide range of communication applications [30–32]. However, the advantages of these systems remain fundamentally limited by their classical nature, particularly in terms of noise resilience, latency, and system complexity.

These limitations open the door to exploring alternative paradigms, particularly those based on quantum principles. While significant progress has been made in entanglement-based quantum MIMO communication methods, such as MIMO-enabled quantum telepor-

tation and QKD [33], these approaches primarily focus on leveraging quantum entanglement for secure information exchange. These studies have provided valuable insights into the integration of MIMO techniques within quantum communication systems. Table 1 summarizes the major existing applications of MIMO in quantum communication, along with their advantages and disadvantages. Notably, all existing works have been proposed with a focus on security using quantum entanglement, while our approach leverages quantum superposition to enable high-fidelity transmission.

However, the specific role of MIMO in quantum superposition-based systems, particularly for media transmission tasks such as image and video delivery, remains largely unexplored. This gap underscores the need to investigate how quantum MIMO architectures that leverage superposition can enhance multimedia delivery under realistic channel conditions. While quantum superposition holds significant promise for improving communication capacity and robustness, its effectiveness in mitigating fading effects, especially for visual content, still requires deeper exploration to advance practical and high-performance quantum communication systems.

Table 1. Summary of MIMO Applications in Quantum Communication Systems.

Reference	Model	Advantages	Limitations
[34]	Entanglement Distribution in spatial multipath channels	Enables secure data transfer	Only limit for the security and high entanglement complexity
[35]	Quantum teleportation MIMO	Improve the throughput and reliability of the quantum channel	Limited data rates
[36]	QKD with MIMO architecture	Enhanced security	Complexity overhead
[37]	MIMO architecture for digital communications	Spatial diversity gain	Measurement alignment sensitivity
[38]	Diversity and multiplexing	Quantum diversity multiplexing tradeoff, robustness via imperfect cloning	Cloning-induced fidelity loss, complexity in channel modeling
[39]	QKD with MIMO architecture	Robust against eavesdropping, higher secret key rate	High path loss at THz frequencies, hardware complexity with multiple antennas
[40]	QKD with MIMO architecture	Ultrawide bandwidth for high-capacity communication, Enhanced secret key rate	Complex and costly hardware, challenging practical deployment in non-laboratory environments
[41]	MIMO quantum communication in pure-loss channels	Improved transmission fidelity	Cloning fidelity constraints, limited scalability

Therefore, this research introduces a novel direction in quantum communication by exploring the use of MIMO techniques using quantum superposition-based systems for video transmission. Unlike traditional approaches, which often overlook media-specific requirements, the proposed method aims to improve the reliability and efficiency of transmitting high-resolution video content across realistic, noise-prone communication channels. By harnessing the advantages of both MIMO and quantum superposition, this work seeks to enhance transmission quality while reducing error rates. The outcome has the potential to significantly advance quantum communication technologies, offering a foundation for practical, high-performance multimedia delivery in future communication networks.

3. Methodology

This section outlines the proposed framework for video transmission over a quantum MIMO communication system, as illustrated in Figure 1. Initially, input videos are compressed using source-encoding techniques to extract their corresponding bitstreams. For simulation purposes, the Versatile Video Coding (VVC) standard [42] is used through the VVenC encoder [43]. The system is evaluated using videos in the YUV420 format, covering various spatial resolutions (320 × 180, 1280 × 720, 1920 × 1080), frame rates (20, 30, and 50 fps), and different sizes of Group of Pictures (GOP) (8, 16, and 32) to thoroughly analyze performance under various conditions. Once the video bitstreams are generated, they undergo channel encoding using polar codes with a code rate of 1/2. These channel-encoded bitstreams are then transformed into quantum superposition states through a quantum encoder. Transmission is carried out over quantum MIMO channels using various diversity configurations, including MISO, SIMO, and SISO setups, as shown in Figure 2, all under Rayleigh fading conditions typical of quantum noisy environments. At the receiver, the quantum decoder first converts the received superposition states back into classical bitstreams. These classical bits are subsequently channel-decoded using the polar decoder and finally passed through the source decoder to reconstruct the original video frames. The performance of the proposed system is benchmarked against a classical MIMO communication system operating at the same bandwidth and under identical diversity scenarios.

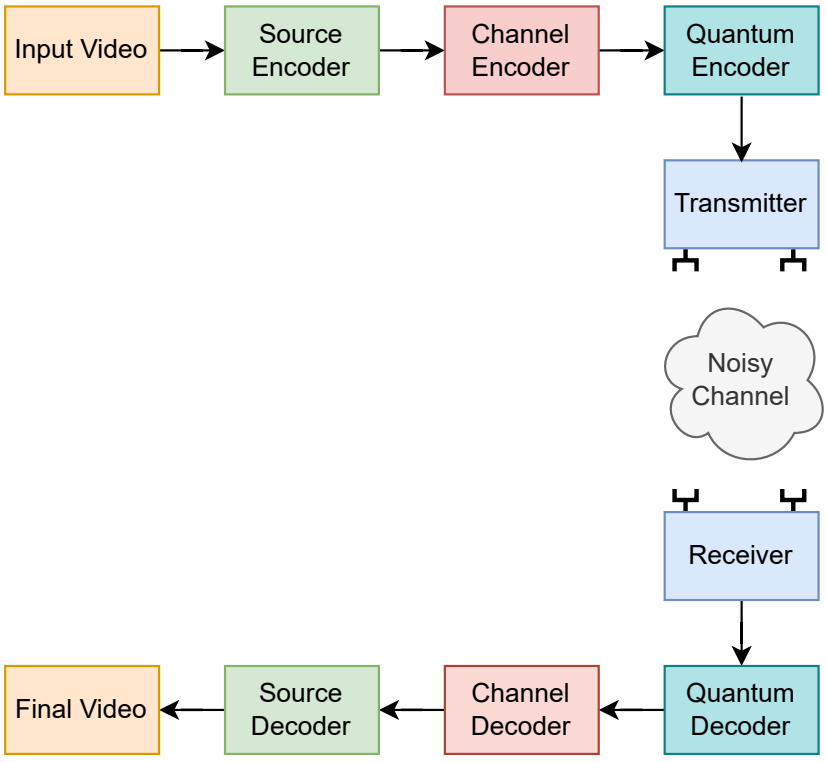

Figure 1. The proposed quantum MIMO communication system.

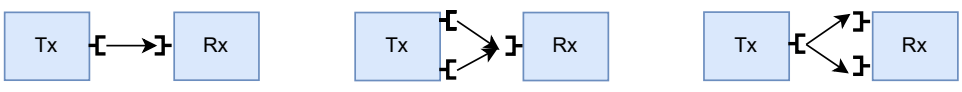

(**a**) 1×1 SISO (**b**) 2×1 MISO (**c**) 1×2 SIMO

Figure 2. MIMO-based diversity schemes employed in simulations: (**a**) No diversity (reference case), (**b**) Transmit diversity, (**c**) Receive diversity.

The following subsections provide detailed descriptions of each functional block within the proposed methodology.

3.1. Video Source Encoding

Input videos are encoded using the VVC standard via the VVenC encoder. The encoder compresses raw YUV420-format videos to reduce bandwidth without significant visual degradation. Experiments are conducted using the following parameters:

- Resolutions: 320×180, 1280×720, 1920×1080
- Frame rates: 20, 30, and 50 fps
- GOP sizes: 8, 16, and 32

The compressed output is a binary bitstream, which can be represented as Equation (1).

$$\mathbf{b} = \{b_1, b_2, ..., b_N\}, \quad b_i \in \{0, 1\} \tag{1}$$

3.2. Channel Encoding Using Polar Codes

The bitstream b is channel-encoded using rate 1/2 polar codes [44] to generate a codeword, where the input vector consists of both information and frozen bits. Polar codes are chosen for their low computational complexity and strong performance in achieving channel capacity under successive cancellation decoding. These characteristics make them highly suitable for both classical and quantum communication systems.

Compared to other classical error correction codes, such as low density parity check (LDPC) codes, turbo codes, or convolutional codes, polar codes offer a more structured and recursive design based on the concept of channel polarization. Polar codes are considered among the most advanced and strong error correction codes currently available. This design enables efficient encoding and decoding, especially in hardware-constrained environments. Moreover, many conventional error-correction codes are tailored to classical, memoryless channels. As a result, those models can lead to increased complexity or suboptimal performance. Polar codes, by contrast, provide a more adaptable and computationally efficient solution, making them a compelling choice in emerging quantum-enhanced communication frameworks.

3.3. Quantum Encoder

The quantum encoder converts channel-encoded classical bits into quantum superposition states. First, if the classical bit is 0, it is mapped to the quantum state $|0\rangle$. If the classical bit is 1, it is mapped to the quantum state $|1\rangle$. After that, a Hadamard gate is applied to each qubit to convert it into a superposition state. Each step of the process is described in detail in the following subsections.

3.3.1. Quantum Bit Mapping

Each classical bit $c_i \in \{0, 1\}$ from the polar-encoded codeword is first mapped to a quantum state in the computational basis, as in Equations (2) and (3).

$$0 \rightarrow |0\rangle = \begin{pmatrix} 1 \\ 0 \end{pmatrix} \tag{2}$$

$$1 \rightarrow |1\rangle = \begin{pmatrix} 0 \\ 1 \end{pmatrix} \tag{3}$$

This step initializes each qubit in a pure basis state, representing classical bits in quantum form.

3.3.2. Hadamard Gate for Superposition

The Hadamard gate (H) is a fundamental single-qubit quantum gate that is used to create superposition. It transforms the computational basis states $|0\rangle$ and $|1\rangle$ into equal superpositions, enabling quantum parallelism [45]. The matrix representation of the Hadamard gate is shown in Equation (4).

$$H = \frac{1}{\sqrt{2}} \begin{pmatrix} 1 & 1 \\ 1 & -1 \end{pmatrix} \tag{4}$$

The Hadamard transform operates on the basis states as in Equations (5) and (6).

$$H|0\rangle = \frac{1}{\sqrt{2}}(|0\rangle + |1\rangle) \tag{5}$$

$$H|1\rangle = \frac{1}{\sqrt{2}}(|0\rangle - |1\rangle) \tag{6}$$

These transformations prepare the qubit in a coherent superposition, which is essential for achieving quantum parallelism in quantum information processing.

3.3.3. Phase Gate for Complex Modulation

In MIMO communication systems, the use of complex baseband modulation requires incorporating phase information into the quantum states. To achieve this, a phase gate (S), defined in Equation (7), is applied to the superposition states generated. This operation enables the integration of phase components essential for representing complex modulated signals.

$$S = \begin{bmatrix} 1 & 0 \\ 0 & i \end{bmatrix} \tag{7}$$

The combined operation (Hadamard + phase) produces the following quantum states as in Equations (8) and (9).

$$\psi_0 = SH|0\rangle = \frac{1}{\sqrt{2}}(|0\rangle + i|1\rangle) \tag{8}$$

$$\psi_1 = SH|1\rangle = \frac{1}{\sqrt{2}}(|0\rangle - i|1\rangle) \tag{9}$$

This encoding strategy is fundamental for enabling complex-valued quantum modulation, which is essential for high-fidelity quantum MIMO communication systems. It allows each qubit to carry more information, analogous to modulated carriers in classical communication systems.

3.4. Quantum MIMO Transmission and Quantum Channel

The qubit states are transmitted using various MIMO diversity schemes: SISO (1×1), MISO (2×1), and SIMO (1×2). Each link experiences Rayleigh flat fading [46], modeled according to the Equation (10).

$$y = h \cdot \psi + n_q \tag{10}$$

where h is a complex channel coefficient, ψ is the superposition state and n_q represents quantum noise. Rayleigh flat fading is a widely used statistical model that characterizes the impact of multipath propagation in non-line-of-sight wireless environments. Under this model, the channel coefficient h is treated as a circularly symmetric complex Gaussian random variable with zero mean and unit variance, i.e., $h \sim \mathcal{CN}(0, 1)$. The term "flat fading" implies that the fading is frequency non-selective; that is, all frequency components of

the transmitted signal experience the same channel gain, which is valid when the signal bandwidth is smaller than the coherence bandwidth of the channel.

The 2×2 MIMO diversity is not considered in this study, as the objective is to independently analyze the impact of transmit (MISO) and receive (SIMO) diversity on the performance of quantum video transmission.

The channel fading parameters are modeled as follows.

- Path delays: $0, 3, 8, 20$ µs
- Path gains: $0, -3, -6, -9$ dB
- Doppler shift: 10 Hz
- Sample rate: 1000 Hz
- SNR range: -3 dB to 19 dB

To assess the performance of the proposed quantum communication system, simulations are conducted using widely accepted and generalized quantum noise models, including bit-flip, phase-flip, depolarizing, amplitude damping, and phase damping channels. These noise models abstract the most fundamental error types encountered in quantum systems and are commonly used in theoretical and simulation-based studies of quantum communication [47,48].

Although more complex hardware-specific imperfections, such as gate errors, leakage, or crosstalk, can affect real-world implementations, they are not considered here. Instead, this work focuses on analyzing the behavior of the core quantum channel under standard noise assumptions to ensure general applicability and theoretical clarity.

To understand the behavior of the noise models applied in this study, it is essential to define the Pauli operators [45], which represent the fundamental quantum error operations. These matrices, known as the Pauli-X (Equation (11)), Pauli-Y (Equation (12)), and Pauli-Z (Equation (13)) operators, are used throughout quantum information theory to model bit-flip, phase-flip, and depolarizing errors.

$$X = \begin{pmatrix} 0 & 1 \\ 1 & 0 \end{pmatrix} \tag{11}$$

$$Y = \begin{pmatrix} 0 & -i \\ i & 0 \end{pmatrix} \tag{12}$$

$$Z = \begin{pmatrix} 1 & 0 \\ 0 & -1 \end{pmatrix} \tag{13}$$

The following subsection describes the various noise models used in this study.

3.4.1. Bit-Flip Noise

Bit-flip noise introduces errors similar to classical bit errors by randomly flipping the state of a qubit from $|0\rangle$ to $|1\rangle$ or vice versa. The likelihood of such an error occurring is denoted by p_x, and its impact on a quantum state ρ is described by Equation (14).

$$\mathcal{N}_X(\rho) = p_x X \rho X^\dagger + (1 - p_x)\rho \tag{14}$$

Here, X is the Pauli-X operator, responsible for flipping the qubit state.

3.4.2. Phase-Flip Noise

Phase-flip noise alters the relative phase of a qubit without changing its probability amplitudes in the computational basis. It is modeled using the Pauli-Z operator with error probability p_z, as shown in Equation (15).

$$\mathcal{N}_Z(\rho) = p_z Z\rho Z^\dagger + (1 - p_z)\rho \tag{15}$$

3.4.3. Depolarizing Noise

Depolarizing noise simulates a complete loss of quantum information by mixing the input state with the maximally mixed state. With depolarization probability p_d, the qubit is affected by random Pauli errors (that is, X, Y, or Z) according to Equation (16).

$$\mathcal{N}_D(\rho) = (1 - p_d)\rho + \frac{p_d}{3}\left(X\rho X^\dagger + Y\rho Y^\dagger + Z\rho Z^\dagger\right) \tag{16}$$

This model uniformly distributes noise across all three Pauli operators, X, Y, and Z.

3.4.4. Amplitude Damping Noise

Amplitude damping reflects energy-loss mechanisms common in physical quantum systems, such as spontaneous emission. It is defined using Kraus operators and is governed by amplitude damping probability p_A, as in Equation (17).

$$\mathcal{N}_A(\rho) = K_0\rho K_0^\dagger + K_1\rho K_1^\dagger \tag{17}$$

The corresponding Kraus operators are represented in Equation (18).

$$K_0 = \begin{pmatrix} 1 & 0 \\ 0 & \sqrt{1 - p_A} \end{pmatrix}, \quad K_1 = \begin{pmatrix} 0 & \sqrt{p_A} \\ 0 & 0 \end{pmatrix} \tag{18}$$

These Kraus operators provide a mathematical framework for describing the effect of noise and decoherence on quantum states in an open quantum system. Any quantum noise channel $\mathcal{N}$ acting on a density matrix ρ can be represented as a set of Kraus operators $\{K_i\}$, which satisfy the completeness relation as in Equation (19).

$$\sum_i K_i^\dagger K_i = I \tag{19}$$

where I is the identity operator. The action of the noise channel on ρ is given by Equation (20).

$$\mathcal{N}(\rho) = \sum_i K_i\rho K_i^\dagger \tag{20}$$

Each Kraus operator K_i represents one possible way the environment can affect the quantum state. This approach is commonly used to describe different types of quantum noise, such as amplitude damping and phase damping.

3.4.5. Phase Damping Noise

Phase damping (or dephasing) captures the loss of quantum coherence without affecting population probabilities. This is particularly relevant in systems where environmental interactions degrade phase information. The noise model is described in Equation (21).

$$\mathcal{N}_P(\rho) = L_0\rho L_0^\dagger + L_1\rho L_1^\dagger \tag{21}$$

The Kraus operators are represented in Equation (22).

$$L_0 = \begin{pmatrix} 1 & 0 \\ 0 & \sqrt{1-p_P} \end{pmatrix}, \quad L_1 = \begin{pmatrix} 0 & 0 \\ 0 & \sqrt{p_P} \end{pmatrix} \tag{22}$$

3.4.6. Combined Noise Model

To simulate more realistic quantum environments, the individual noise channels are aggregated into a composite model. The overall effect on a quantum state is given by Equation (23).

$$\mathcal{N}(\rho) = p_X\mathcal{N}_X(\rho) + p_Z\mathcal{N}_Z(\rho) + p_D\mathcal{N}_D(\rho) + p_A\mathcal{N}_A(\rho) + p_P\mathcal{N}_P(\rho) \tag{23}$$

In all equations, $\mathcal{N}(\rho)$ denotes the output noisy state, ρ is the initial quantum density matrix, and X, Y, Z are standard Pauli operators. The dagger symbol (†) indicates the Hermitian conjugate. By randomly adjusting individual noise probabilities based on the channel SNR, the performance of the system can be rigorously tested under a variety of realistic channel conditions.

3.5. Quantum Decoding and Measurement

At the receiver, the applied phase shift from the quantum encoder is first reversed using the inverse phase gate $S^\dagger$, defined as in Equation (24).

$$S^\dagger = \begin{bmatrix} 1 & 0 \\ 0 & -i \end{bmatrix} \tag{24}$$

This operation restores the original phase of the superposition state of the qubit, which is necessary to recover the transmitted information. Once the inverse phase operation is applied, the receiver can perform a measurement on the computational basis using the common projection operators defined in Equation (25).

$$M_0 = |0\rangle\langle 0|, \quad M_1 = |1\rangle\langle 1| \tag{25}$$

Each measurement operator can be applied to the quantum states received $|\psi_0\rangle = \frac{1}{\sqrt{2}}(|0\rangle + |1\rangle)$ and $|\psi_1\rangle = \frac{1}{\sqrt{2}}(|0\rangle - |1\rangle)$. Then, the normalized post-measurement state can be calculated using Equation (26).

$$|\psi'\rangle = \frac{M_m|\psi\rangle}{\sqrt{\langle\psi| M_m^\dagger M_m |\psi\rangle}} \tag{26}$$

Case 1: Applying M_0
For $|\psi_0\rangle$:

$$|\psi'\rangle = \frac{|0\rangle\langle 0|\left(\frac{1}{\sqrt{2}}|0\rangle + \frac{1}{\sqrt{2}}|1\rangle\right)}{\sqrt{\left(\frac{1}{\sqrt{2}}\langle 0| + \frac{1}{\sqrt{2}}\langle 1|\right)(|0\rangle\langle 0|)\left(\frac{1}{\sqrt{2}}|0\rangle + \frac{1}{\sqrt{2}}|1\rangle\right)}} \tag{27}$$

$$= |0\rangle \tag{28}$$

For $|\psi_1\rangle$:

$$|\psi'\rangle = \frac{|0\rangle\langle 0|\left(\frac{1}{\sqrt{2}}|0\rangle - \frac{1}{\sqrt{2}}|1\rangle\right)}{\sqrt{\left(\frac{1}{\sqrt{2}}\langle 0| - \frac{1}{\sqrt{2}}\langle 1|\right)(|0\rangle\langle 0|)\left(\frac{1}{\sqrt{2}}|0\rangle - \frac{1}{\sqrt{2}}|1\rangle\right)}} \tag{29}$$

$$= |0\rangle \tag{30}$$

In this case (Case 1), applying M_0 to both superposition states results in the same output $|0\rangle$, as shown in Equations (27)–(30). Therefore, this measurement does not reveal any information about the original transmitted superposition state, making it impossible to distinguish whether the received state is $|\psi_0\rangle$ or $|\psi_1\rangle$.

Case 2: Applying M_1

For $|\psi_0\rangle$:

$$|\psi'\rangle = \frac{|1\rangle\langle 1|\left(\frac{1}{\sqrt{2}}|0\rangle + \frac{1}{\sqrt{2}}|1\rangle\right)}{\sqrt{\left(\frac{1}{\sqrt{2}}\langle 0| + \frac{1}{\sqrt{2}}\langle 1|\right)(|1\rangle\langle 1|)\left(\frac{1}{\sqrt{2}}|0\rangle + \frac{1}{\sqrt{2}}|1\rangle\right)}} \tag{31}$$

$$= |1\rangle \tag{32}$$

For $|\psi_1\rangle$:

$$|\psi'\rangle = \frac{|1\rangle\langle 1|\left(\frac{1}{\sqrt{2}}|0\rangle - \frac{1}{\sqrt{2}}|1\rangle\right)}{\sqrt{\left(\frac{1}{\sqrt{2}}\langle 0| - \frac{1}{\sqrt{2}}\langle 1|\right)(|1\rangle\langle 1|)\left(\frac{1}{\sqrt{2}}|0\rangle - \frac{1}{\sqrt{2}}|1\rangle\right)}} \tag{33}$$

$$= -|1\rangle \tag{34}$$

Unlike M_0, applying M_1 reveals a phase difference in the resulting quantum state as in Equations (31)–(34). If the result is $|1\rangle$, the original state is $|\psi_0\rangle$, which corresponds to the classical bit 0. If the result is $-|1\rangle$, the original state is $|\psi_1\rangle$, which corresponds to the classical bit 1. This phase-based discrimination allows the receiver to correctly identify the transmitted superposition state. By observing the sign of the qubit state ($+$ or $-$) in the post-measurement state under M_1, the receiver can reliably extract the classical bitstream from the measured quantum states.

3.6. Channel Decoding and Source Decoding to Video Reconstruction

The extracted classical bitstream from the superposition states is recovered via polar decoding, followed by VVC decoding to reconstruct the original video. This marks the completion of the end-to-end quantum video transmission process.

3.7. Simulation Environment

Simulations are performed using Python 3 on a computer system with the following features.

- CPU: Intel Core i5-1345U, 1.60 GHz (Intel Corporation, Santa Clara, CA, USA)
- RAM: 16 GB

In addition, the model assumes the perfect channel state information (CSI) at the receiver, ensuring optimal decoding performance and mitigating errors caused by uncertain channel conditions. To enable fair comparison, the classical MIMO system uses complex baseband binary phase shift keying (BPSK) modulation with rate $1/2$ polar coding, matching the bandwidth usage of the proposed quantum system. For statistical robustness,

the evaluation is conducted by subjecting each video to 1000 transmission trials. The results presented reflect the average performance across all trials, measured using the PSNR, SSIM, and VMAF metrics.

4. Results and Discussion

This study evaluates the performance of a superposition-based quantum communication system for video transmission in three diversity configurations: 1×1 SISO, 2×1 MISO, and 1×2 SIMO. Instead of varying GOP sizes, the evaluation is based on three representative video sequences selected for their differing levels of structural information (SI) and temporal information (TI), corresponding to high-motion, medium-motion, and low-motion characteristics. High-motion video [49] is characterized by rapid object movement and frequent scene transitions, resulting in high SI and TI values. This makes compression and transmission particularly challenging. The medium-motion video [50] exhibits moderate changes in scene and movement, leading to balanced SI and TI levels, and representing an average complexity case. In contrast, low-motion video [51] features relatively static scenes with minimal movement, producing moderate SI but low TI, making it the easiest to compress and transmit. Due to the use of three distinct video sequences, the final performance metrics are reported as the average values across all three types. This approach ensures a comprehensive evaluation of the effectiveness of the system under various content conditions.

As shown in Figure 3, the PSNR, SSIM, and VMAF values of the decoded videos are plotted against the channel SNR for a GOP size of 8, a resolution of 320×180, and a frame rate of 50 fps. The results indicate that the quantum system (Q) consistently achieves superior video quality, measured by PSNR, SSIM, and VMAF, compared to the classical system (C), particularly under low-SNR conditions across all diversity configurations, including MISO, SIMO, and SISO. The quantum system demonstrates that increasing channel noise results in more frequent quantum state errors during transmission. These errors are subsequently converted into classical bit errors during decoding, causing visible distortions and reducing the perceptual quality of the reconstructed video.

In addition, both the MISO (transmit diversity) and SIMO (receive diversity) configurations outperform the SISO (no diversity) scheme in terms of video transmission quality in both quantum and classical systems. This advantage is most evident in the 2×1 MISO and 1×2 SIMO quantum setups, where the quantum system maintains strong video quality, as in PSNR results at SNR levels as low as 7 dB. In contrast, the 1×1 SISO configuration requires a minimum of 10 dB SNR to achieve comparable performance. This performance gap underscores the benefit of using diversity techniques in conjunction with quantum encoding to enhance communication robustness. The improved resilience to noise enables more accurate video reconstruction even in challenging channel conditions. A similar trend is observed in the SSIM and VMAF results, further confirming the superior perceptual and structural quality delivered by the quantum-enhanced transmission framework across all diversity schemes. It is also observed that the 2×1 MISO setup exhibits around a 3 dB performance drop relative to the 1×2 SIMO scheme in both the classical and quantum cases. This reduction is due to the experiments being configured with equal total transmission power across all configurations, which inherently benefits receive diversity.

As illustrated in Figure 4, the PSNR, SSIM, and VMAF results for a GOP size of 16 follow a similar trend to those observed with a GOP size of 8. In all diversity configurations, including MISO, SIMO, and SISO, the quantum system continues to outperform the classical system. Additionally, both transmit (2×1 MISO) and receive diversity (1×2 SIMO) provide better results compared to the no diversity (1×1 SISO) scheme. However, a no-

ticeable drop in overall performance is observed when the GOP size increases from 8 to 16.

To further investigate this behavior, Figure 5 presents the results for a GOP size of 32. While the quantum system continues to outperform its classical counterpart, and MISO and SIMO configurations show better results than SISO, the overall video quality is reduced compared to that achieved with a GOP size of 16. The reason is that, as the GOP size increases, more frames are encoded using inter-frame prediction. Since these frames depend on preceding intra and inter-coded frames within the same GOP, any error introduced partway through can propagate and severely impact the quality of the remaining predicted frames. This trend is evident in Figures 3–5, where performance metrics progressively decrease as the GOP size grows from 8 to 16 and further to 32. Therefore, to maintain consistent video quality in these scenarios, it is essential to adopt adaptive error-correction techniques that dynamically allocate protection based on the GOP frame hierarchy. Coupling these methods with error-resilient video-encoding approaches, such as flexible macroblock ordering or intra-refresh strategies, can help localize errors and prevent widespread quality degradation. These combined solutions offer a promising direction to improve robustness in video transmission over quantum and classical channels alike.

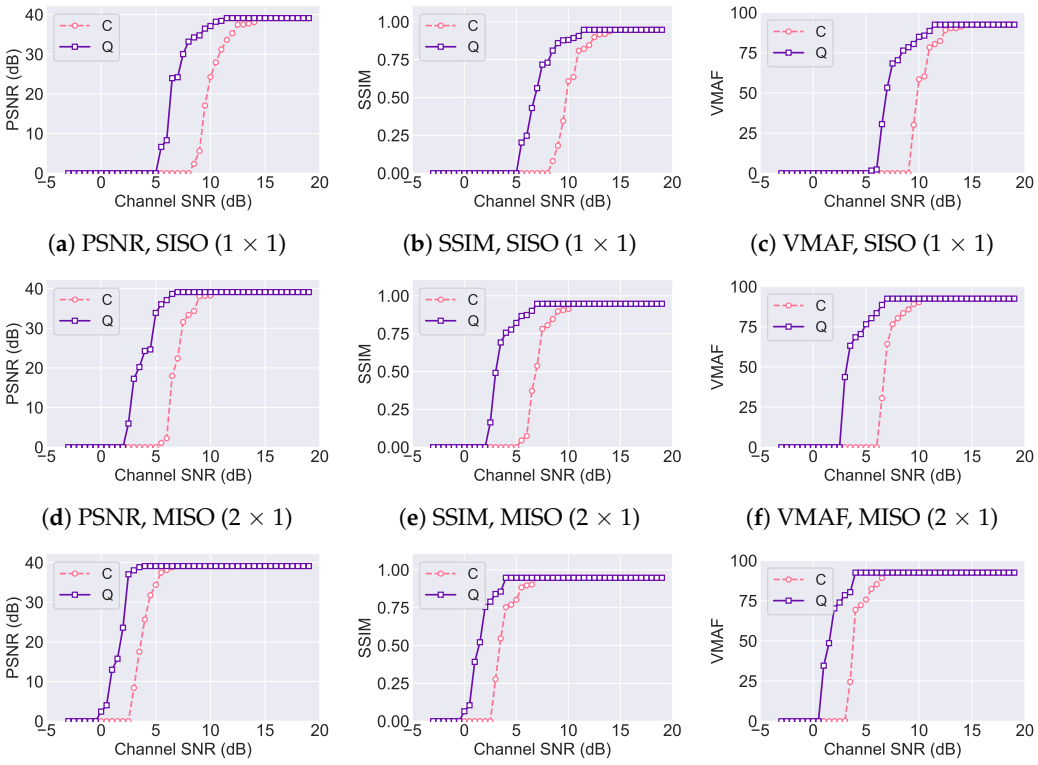

(**a**) PSNR, SISO (1 × 1) (**b**) SSIM, SISO (1 × 1) (**c**) VMAF, SISO (1 × 1)

(**d**) PSNR, MISO (2 × 1) (**e**) SSIM, MISO (2 × 1) (**f**) VMAF, MISO (2 × 1)

(**g**) PSNR, SIMO (1 × 2) (**h**) SSIM, SIMO (1 × 2) (**i**) VMAF, SIMO (1 × 2)

Figure 3. Comparison of average PSNR (**left column**), SSIM (**center column**), and VMAF (**right column**) for classical (C) and quantum (Q) systems across diversity schemes: (**a**–**c**) 1 × 1 SISO, (**d**–**f**) 2 × 1 MISO, and (**g**–**i**) 1 × 2 SIMO with GOP size 8.

Furthermore, transmit (MISO) and receive (SIMO) diversity schemes enhance system robustness by mitigating the adverse effects of signal degradation in both classical and quantum communication systems. In classical systems, diversity techniques primarily address channel fading caused by multipath propagation and interference. These methods help improve signal quality and reliability by combining multiple signal paths at the receiver. In quantum systems, however, the communication channel is also affected by unique impairments such as quantum noise, decoherence, and quantum fading, phenomena that

do not exist in classical transmission. While classical fading impacts the amplitude and phase of transmitted signals, quantum fading and noise can disrupt the delicate superposition states essential for quantum communication. Despite these challenges, diversity schemes such as MISO and SIMO still contribute to performance improvements in quantum systems by increasing redundancy and reception reliability. Moreover, the use of quantum superposition further enhances the system's ability to resist quantum impairments. By representing multiple bit states simultaneously, quantum encoding allows information to be distributed across parallel quantum states, making the system inherently more tolerant to noise and fading. As a result, quantum-enhanced systems demonstrate superior resilience and reconstruction accuracy, especially in low-SNR scenarios, as confirmed by PSNR, SSIM, and VMAF metrics across different diversity schemes and GOP sizes.

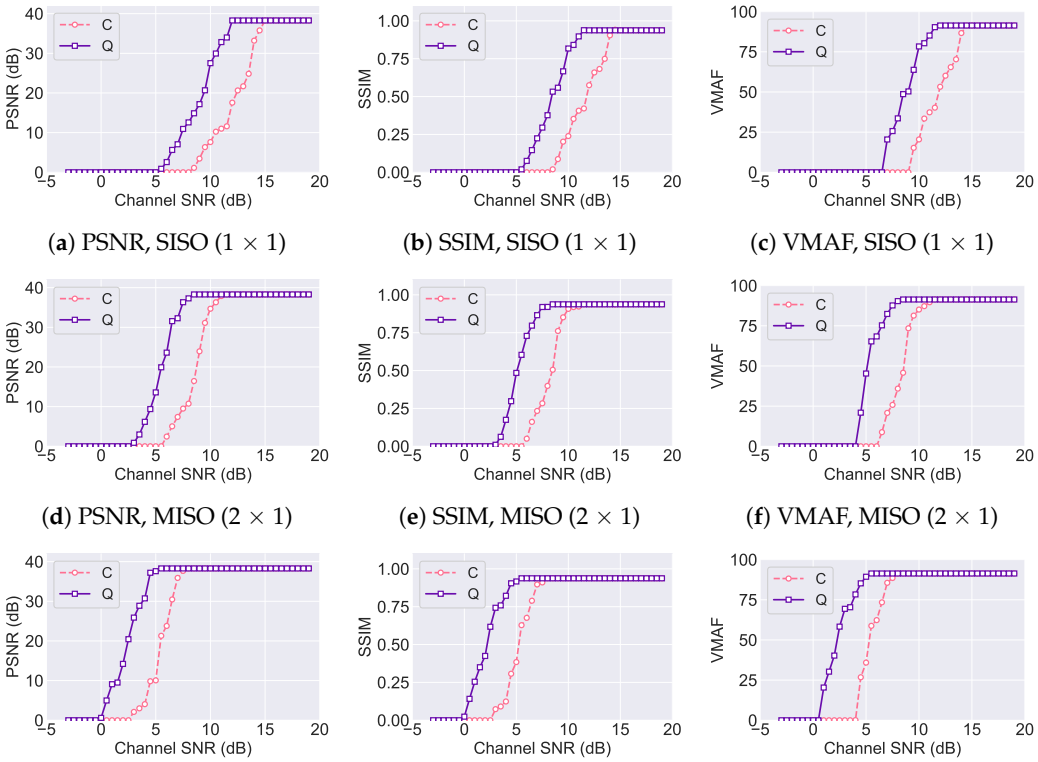

(**a**) PSNR, SISO (1 × 1) (**b**) SSIM, SISO (1 × 1) (**c**) VMAF, SISO (1 × 1)

(**d**) PSNR, MISO (2 × 1) (**e**) SSIM, MISO (2 × 1) (**f**) VMAF, MISO (2 × 1)

(**g**) PSNR, SIMO (1 × 2) (**h**) SSIM, SIMO (1 × 2) (**i**) VMAF, SIMO (1 × 2)

Figure 4. Comparison of average PSNR (**left column**), SSIM (**center column**), and VMAF (**right column**) for classical (C) and quantum (Q) systems across diversity schemes: (**a**–**c**) 1 × 1 SISO, (**d**–**f**) 2 × 1 MISO, and (**g**–**i**) 1 × 2 SIMO with GOP size 16.

In addition, the impact of varying frame rates and resolutions on the performance of the proposed quantum MIMO communication system is evaluated, with GOP size 8 selected as a representative test case, as summarized in Table 2. The comparative analysis demonstrates that variations in resolution and frame rate have minimal effect on the maximum channel SNR gains achieved by the quantum system compared to the classical baseline. This channel SNR gain is quantified using Equation (35).

$$\Delta\mathrm{SNR}(Q) = \mathrm{SNR}_{\mathrm{classical}}(Q) - \mathrm{SNR}_{\mathrm{quantum}}(Q) \tag{35}$$

where $\mathrm{SNR}_{\mathrm{classical}}(Q)$ and $\mathrm{SNR}_{\mathrm{quantum}}(Q)$ denote the channel SNR values required by the baseline and proposed systems, respectively, to achieve the same quality level Q. The consistency of the results indicates that both quantum and classical communication systems respond similarly to changes in these video parameters. The results imply that

improvements offered by the quantum approach are robust across different video formats and playback speeds. Consequently, the performance advantages of the quantum system can be expected to hold under a wide range of practical video streaming conditions, supporting its applicability in various real-world scenarios. These findings also highlight the scalability and flexibility of the proposed quantum communication framework when handling video content of varying complexities and qualities.

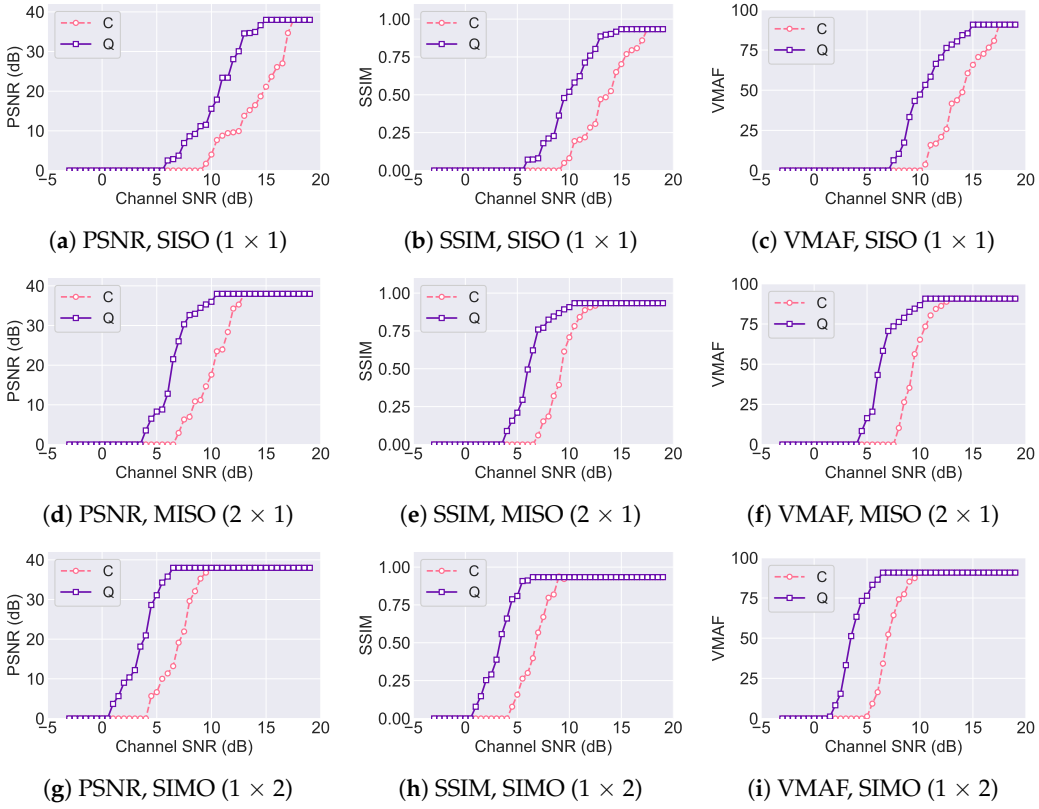

(**a**) PSNR, SISO (1 × 1) (**b**) SSIM, SISO (1 × 1) (**c**) VMAF, SISO (1 × 1)

(**d**) PSNR, MISO (2 × 1) (**e**) SSIM, MISO (2 × 1) (**f**) VMAF, MISO (2 × 1)

(**g**) PSNR, SIMO (1 × 2) (**h**) SSIM, SIMO (1 × 2) (**i**) VMAF, SIMO (1 × 2)

Figure 5. Comparison of average PSNR (**left column**), SSIM (**center column**), and VMAF (**right column**) for classical (C) and quantum (Q) systems across diversity schemes: (**a**–**c**) 1 × 1 SISO, (**d**–**f**) 2 × 1 MISO, and (**g**–**i**) 1 × 2 SIMO with GOP size 32.

Table 2. Maximum SNR gain for each diversity scheme of the quantum communication system compared to the corresponding diversity scheme of the classical communication system across different resolutions and frame rates.

Frame Rate (fps)	1280 × 720			1920 × 1080		
	1 × 1	**2 × 1**	**1 × 2**	**1 × 1**	**2 × 1**	**1 × 2**
20	3.0 dB	3.0 dB	3.1 dB	3.0 dB	2.8 dB	3.0 dB
30	3.0 dB	2.9 dB	3.0 dB	3.0 dB	3.0 dB	3.0 dB
50	3.0 dB	3.1 dB	3.0 dB	2.8 dB	2.8 dB	3.0 dB

To assess the perceived visual quality of the video content, a subjective evaluation is performed using the double stimulus method [52], involving 80 participants between the ages of 17 and 55. The assessment covers GOP size 8 across three diversity scenarios: SISO, MISO, and SIMO. In this process, video sequences produced by both quantum and classical communication systems are shown, and participants are asked to rate the visual quality of each. The subjective quality scores follow the standard Mean Opinion Score (MOS) convention on a 0–100 scale, where 0–20 indicates bad, 21–40 poor, 41–60 fair, 61–80 good, and 81–100 excellent quality; the reported MOS values represent the average

perceptual ratings across all evaluators. The collected ratings are analyzed and the results are presented in Figure 6 for SISO (1 × 1), Figure 7 for MISO (2 × 1), and Figure 8 for SIMO (1 × 2). A clear alignment is found between subjective ratings and objective metrics such as PSNR, SSIM, and VMAF, confirming the consistency of both evaluation approaches. To further validate the results, a sample of decoded frames for each diversity scenario, as well as for both quantum and classical systems, is presented in Figure 9. Under MISO and SIMO configurations, the images are decoded at an SNR of 7.5 dB. However, under SISO, decoding at SNR 7.5 dB is not possible due to the high BER. Therefore, the decoded frame at an SNR of 10 dB is included for the SISO configuration. Visual inspection of these frames corresponds well to subjective and objective quality metrics, thereby reinforcing the validity of the findings.

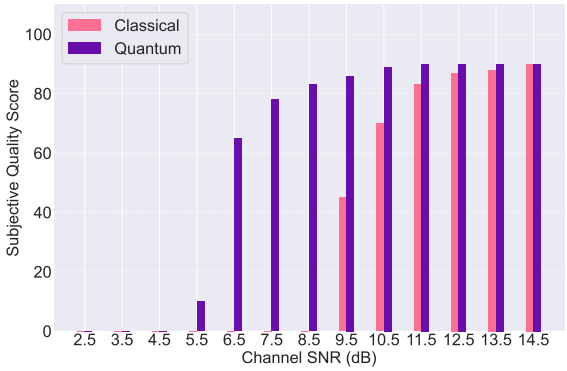

Figure 6. Subjective quality assessment results for VVC-encoded videos with SISO (1 × 1 No Diversity), comparing quantum and classical communication systems for GOP 8.

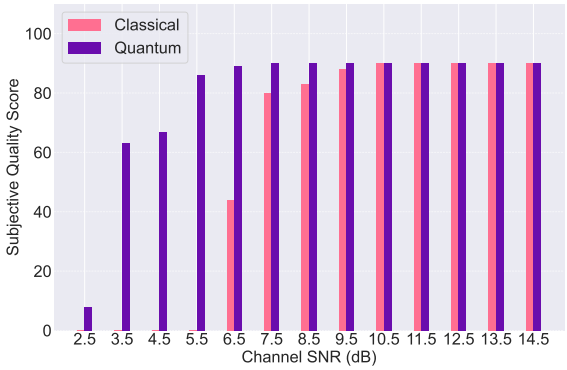

Figure 7. Subjective quality assessment results for VVC-encoded videos with MISO (2 × 1 Transmit Diversity), comparing quantum and classical communication systems for GOP 8.

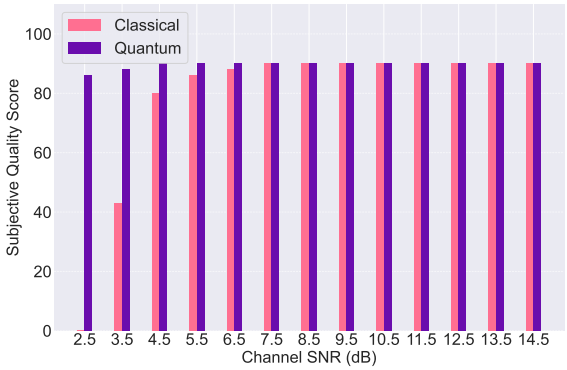

Figure 8. Subjective quality assessment results for VVC-encoded videos with SIMO (1 × 2 Receive Diversity), comparing quantum and classical communication systems for GOP 8.

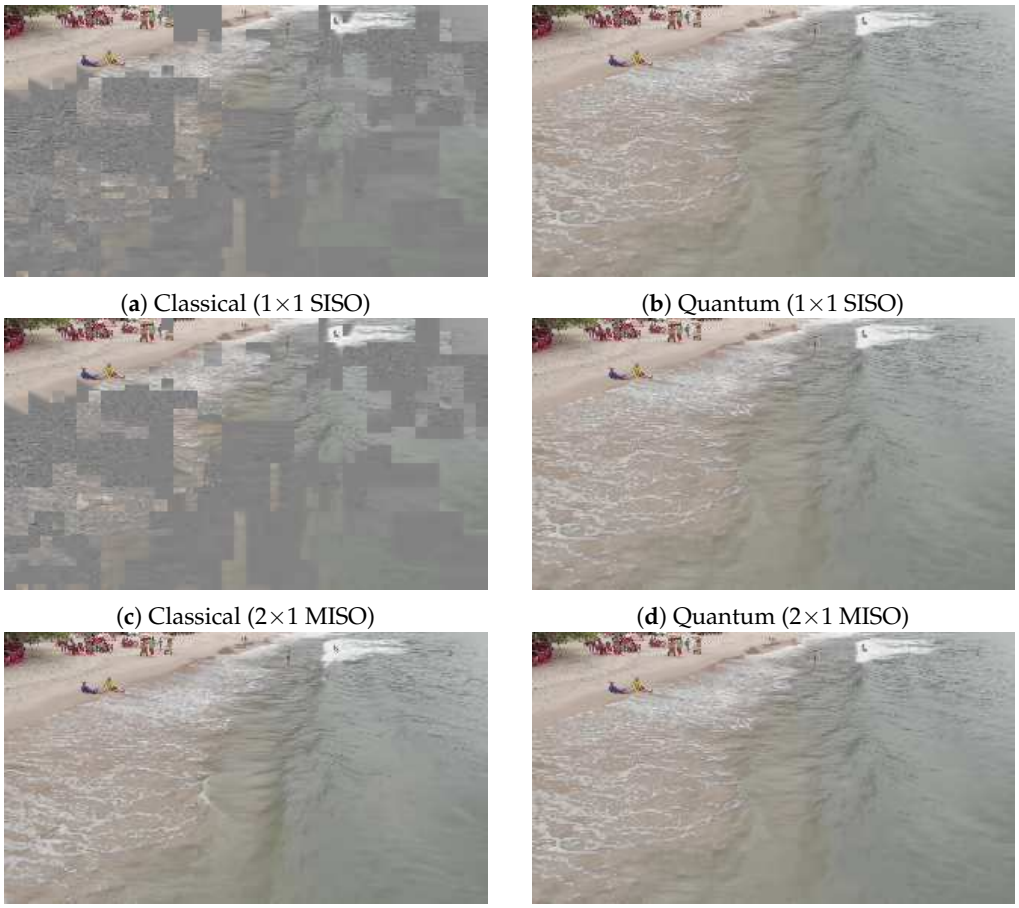

(**a**) Classical (1×1 SISO) (**b**) Quantum (1×1 SISO)

(**c**) Classical (2×1 MISO) (**d**) Quantum (2×1 MISO)

(**e**) Classical (1×2 SIMO) (**f**) Quantum (1×2 SIMO)

Figure 9. Example of a received video frame for classical and quantum systems under different diversity schemes. (**a**,**b**) correspond to 1 × 1 SISO with a channel SNR of 10.5 dB; (**c**,**d**) correspond to 2 × 1 MISO with a channel SNR of 7.5 dB; (**e**,**f**) correspond to 1 × 2 SIMO with a channel SNR of 7.5 dB.

Motivated by the demand for low-complexity systems capable of delivering high visual quality in real-time, this study introduces a hybrid communication framework that integrates classical and quantum technologies. The proposed architecture is designed to support near-real-time implementation while maintaining minimal system complexity, making it well-suited for deployment in resource-constrained environments.

Within the proposed framework, quantum encoding involves applying Hadamard transformations to individual qubits representing bitstream segments, resulting in a computational complexity that scales linearly as $\mathcal{O}(N)$, where N is the number of qubits. Since our system uses single-qubit encoding with $N = 1$, the encoding complexity reduces to a constant $\mathcal{O}(1)$, representing the simplest and most efficient quantum encoding scheme. Similarly, quantum decoding is performed via single-qubit measurements, which also exhibit constant-time complexity $\mathcal{O}(1)$ per qubit. By avoiding entanglement, additional quantum gates beyond Hadamard, and quantum error correction codes, the framework maintains minimal computational and hardware demands.

While classical communication systems benefit from decades of standardization, offering high reliability and sophisticated optimization techniques, quantum systems offer an inherently different advantage: reduced algorithmic and computational complexity rooted in the fundamental properties of quantum hardware. In our design, this advantage is further amplified through the use of single-qubit operations and Hadamard-based quantum modulation, which collectively minimize computational overhead. It is also important to

note that the performance evaluations presented in this work are derived from classical simulations of quantum operations. Since quantum hardware operates very differently from classical processors, especially in how it handles parallelism and state changes, runtime comparisons based on simulations do not accurately reflect the performance of real quantum devices and are not included in this study.

Furthermore, to maintain this low complexity and ensure hardware feasibility, the system intentionally omits quantum error correction (QEC) techniques [53]. While QEC methods can improve error resilience, they typically introduce substantial computational and implementation overheads, making them impractical for near-term, scalable, and low-power deployments, especially in MIMO-based scenarios. While the proposed design avoids QEC to reduce complexity, we acknowledge that its absence increases vulnerability to decoherence and cumulative noise in practical quantum channels. However, for low-complexity, short-distance communication scenarios, the use of classical polar codes has proven sufficient to maintain reliable performance.

Although the proposed system is evaluated through simulation, this process serves as a foundational step toward practical validation. The results aim to guide future efforts, including prototype development, experimental testing, and controlled laboratory trials. In the analysis a 2×2 MIMO configuration is introduced to examine the influence of the diversity of transmit and receive. This configuration is not selected for performance benchmarking alone, but also to demonstrate that the proposed framework can accommodate such diversity structures without requiring significant architectural changes. Importantly, the system is designed to be scalable. It can be extended to higher-order MIMO configurations such as 4×4 or 8×8 depending on the availability of quantum hardware and processing resources. While increased complexity may result from such extensions, the modularity and low baseline complexity of the current design ensure that future expansions are feasible. This scalability positions the proposed quantum-classical hybrid framework as a strong candidate for next-generation communication systems in applications such as telemedicine, remote diagnostics, and real-time visual transmission in bandwidth-limited or error-prone environments.

5. Conclusions and Future Work

This study introduces a quantum MIMO communication framework that aims to enhance the reliable transmission of high-quality video over wireless channels. By combining quantum superposition with classical channel coding and spatial diversity strategies, specifically SISO, MISO, and SIMO configurations within a 2×2 MIMO system, the proposed method effectively mitigates the effects of multipath fading and noise. Specifically, within this framework, compressed video sequences are encoded into quantum superposition states, enabling transmission that is more robust and resilient to fading and quantum noise. The simulation results confirm that the proposed system significantly outperforms the classical counterparts under identical channel and bandwidth conditions. Specifically, the proposed system achieves up to 39.12 dB in PSNR, 0.9471 in SSIM, and 92.47 in VMAF compared to the classical system. These improvements are consistently observed across different GOP sizes, resolutions, and frame rates, demonstrating the framework's flexibility and resilience to temporal compression variations. The architecture is designed for scalability and low complexity, making it suitable for near-future hardware implementation and practical deployment in advanced wireless communication scenarios. Furthermore, this architecture can be extended to any complex MIMO configuration based on the proven results that show promising performance.

Future work will focus on enhancing the scalability of the proposed framework in several directions. First, the MIMO configuration can be extended to higher-order systems

(e.g., 4×4 and beyond), enabling greater spatial diversity and throughput. However, such expansion necessitates the development of low-complexity QEC schemes specifically tailored to quantum MIMO environments. The design of lightweight and hardware-friendly QEC algorithms will be a key research direction to preserve the reliability of the system without compromising efficiency. In addition, machine learning-based CSI prediction techniques will be explored to further optimize performance under dynamic wireless conditions. Integrating machine learning-based CSI estimation with quantum encoding can enable more adaptive and resilient transmission, particularly in highly variable or resource-constrained environments. Moreover, extending the comparison to hybrid classical–quantum frameworks, including edge-assisted video transmission and cross-layer optimization powered by AI, will provide a more comprehensive performance evaluation. These advancements aim to bridge the gap between theoretical quantum communication models and their practical realization, paving the way for efficient, scalable, and intelligent quantum-assisted wireless video transmission systems.

Author Contributions: Conceptualization, U.J.; methodology, U.J.; software, P.S. and T.F.; validation, U.J. and A.F.; formal analysis, A.F.; investigation, A.F.; resources, U.J.; data curation, U.J.; writing—original draft preparation, U.J.; writing—review and editing, T.F.; visualization, U.J.; supervision, A.F.; project administration, A.F. All authors have read and agreed to the published version of the manuscript.

Funding: This research received no external funding.

Data Availability Statement: The original data presented in the study are openly available at https://www.pexels.com under the Creative Commons Zero (CC0) license, which allows free use, distribution, and modification without attribution.

Conflicts of Interest: The authors declare no conflicts of interest.

Abbreviations

ARQ	Automatic Repeat Request
AVC	Advanced Video Coding
AV1	AOMedia Video 1
CSI	Channel State Information
FEC	Forward Error Correction
GOP	Group of Pictures
HD	High-Definition
HEVC	High Efficiency Video Coding
LDPC	Low-Density Parity-Check
MIMO	Multi-Input Multi-Output
MISO	Multi-Input Single-Output
PSNR	Peak Signal-to-Noise Ratio
QEC	Quantum Error Correction
QKD	Quantum Key Distribution
SI	Spatial Information
SIMO	Single-Input Multi-Output
SNR	Signal-to-Noise Ratio
SSIM	Structural Similarity Index Measure
UHD	Ultra-High-Definition
VMAF	Video Multi-Method Assessment Fusion
VP9	Video Processing 9
VVC	Versatile Video Coding
TI	Temporal Information

References

1. Arena, F.; Collotta, M.; Pau, G.; Termine, F. An Overview of Augmented Reality. *Computers* **2022**, *11*, 28. [CrossRef]
2. Hornsey, R.; Hibbard, P. Current Perceptions of Virtual Reality Technology. *Appl. Sci.* **2024**, *14*, 4222. [CrossRef]
3. Wong, E.; Wahab, N.; Saeed, F.; Alharbi, N. 360-Degree Video Bandwidth Reduction: Technique and Approaches Comprehensive Review. *Appl. Sci.* **2022**, *12*, 7581. [CrossRef]
4. Dala Pegorara Souto, V.; Dester, P.; Soares Pereira Facina, M.; Gomes Silva, D.; de Figueiredo, F.; Rodrigues de Lima Tejerina, G.; Silveira Santos Filho, J.; Silveira Ferreira, J.; Mendes, L.; Souza, R.; et al. Emerging MIMO Technologies for 6G Networks. *Sensors* **2023**, *23*, 1921. [CrossRef] [PubMed]
5. Sharma, P.; Tiwari, R.; Singh, P.; Kumar, P.; Kanaujia, B. MIMO Antennas: Design Approaches, Techniques and Applications. *Sensors* **2022**, *22*, 7813. [CrossRef] [PubMed]
6. Yasmineh, S. Foundations of Quantum Mechanics. *Encyclopedia* **2022**, *2*, 1082–1090. [CrossRef]
7. Ralston, J. What Can We Learn from Entanglement and Quantum Tomography? *Physics* **2022**, *4*, 1371–1383. [CrossRef]
8. Ballentine, L.E. *Quantum Mechanics: A Modern Development*, 2nd ed.; World Scientific Publishing Company: Singapore, 2014; p. 740.
9. Zou, N. Quantum Entanglement and Its Application in Quantum Communication. *J. Phys. Conf. Ser.* **2021**, *1827*, 012120. [CrossRef]
10. Sridhar, G.T.; Ashwini, P.; Tabassum, N. A Review on Quantum Communication and Computing. In Proceedings of the 2023 2nd International Conference on Applied Artificial Intelligence and Computing (ICAAIC), Salem, India, 4–6 May 2023; pp. 1592–1596. [CrossRef]
11. Wang, P.; Zhang, X.; Chen, G. Efficient quantum-error correction for QoS provisioning over QKD-based satellite networks. In Proceedings of the 2015 IEEE Wireless Communications and Networking Conference (WCNC), New Orleans, LA, USA, 9–12 March 2015; pp. 2262–2267. [CrossRef]
12. Comi, P.; Martelli, P.; Martin, V.; Brito, J.P.; Gatto, A.; Méndez, R.B.; Vicente, R.J.; Bianchi, F.; Brunero, M. Increasing network reliability by securing SDN communication with QKD. In Proceedings of the 2021 17th International Conference on the Design of Reliable Communication Networks (DRCN), Milano, Italy, 19–22 April 2021; pp. 1–3. [CrossRef]
13. Mamiya, A.; Tanaka, K.; Yokote, S.; Sasaki, M.; Fujiwara, M.; Tanaka, M.; Sato, H.; Katagiri, Y. Satellite-based QKD for Global Quantum Cryptographic Network Construction. In Proceedings of the 2022 IEEE International Conference on Space Optical Systems and Applications (ICSOS), Kyoto City, Japan, 28–31 March 2022; pp. 47–50. [CrossRef]
14. Karthik, M.; Lalwani, J.; Jajodia, B. Quantum Image Teleportation Protocol (QITP) and Quantum Audio Teleportation Protocol (QATP) by using Quantum Teleportation and Huffman Coding. In Proceedings of the 2022 International Conference on Trends in Quantum Computing and Emerging Business Technologies (TQCEBT), Pune, India, 13–15 October 2022; pp. 1–6. [CrossRef]
15. Tan, X.; Jiang, L.; Zhang, Q. Controlled Quantum Teleportation with Identity Authentication. In Proceedings of the 2013 Fourth International Conference on Emerging Intelligent Data and Web Technologies, Xi'an, China, 9–11 September 2013; pp. 350–355. [CrossRef]
16. Johnson, S.; Rarity, J.; Padgett, M. Transmission of quantum-secured images. *Sci. Rep.* **2024**, *14*, 11579. [CrossRef] [PubMed]
17. Janani, T.; Brindha, M. A secure medical image transmission scheme aided by quantum representation. *J. Inf. Secur. Appl.* **2021**, *59*, 102832. [CrossRef]
18. Yamaguchi, T.; Kimura, N.; Mochida, Y.; Mizuno, K.; Takasugi, K.; Chikara, S.; Saito, T.; Shirai, D. Uncompressed 8K-video-transmission System for Remote Production Secured by Post-quantum Cryptography. In Proceedings of the 2023 IEEE International Symposium on Broadband Multimedia Systems and Broadcasting (BMSB), Beijing, China, 14–16 June 2023; pp. 1–6. [CrossRef]
19. Guérin, P.A.; Feix, A.; Araújo, M.; Brukner, Č. Exponential Communication Complexity Advantage from Quantum Superposition of the Direction of Communication. *Phys. Rev. Lett.* **2016**, *117*, 100502. [CrossRef] [PubMed]
20. Feix, A.; Araújo, M.; Brukner, Č. Quantum superposition of the order of parties as a communication resource. *Phys. Rev. A* **2015**, *92*, 052326. [CrossRef]
21. Goswami, K.; Cao, Y.; Paz-Silva, G.A.; Romero, J.; White, A.G. Increasing communication capacity via superposition of order. *Phys. Rev. Res.* **2020**, *2*, 033292. [CrossRef]
22. Jayasinghe, U.; Samarathunga, P.; Ganearachchi, Y.; Fernando, T.; Fernando, A. Quantum communications for image transmission over error-prone channels. *Electron. Lett.* **2024**, *60*, e13300. [CrossRef]
23. Jayasinghe, U.; Samarathunga, P.; Fernando, T.; Ganearachchi, Y.; Fernando, A. Image Transmission Over Quantum Communication Systems With Three-Qubit Error Correction. *Electron. Lett.* **2025**, *61*, e70205. [CrossRef]
24. Jayasinghe, U.; Samarathunga, P.; Pollwaththage, N.; Ganearachchi, Y.; Fernando, T.; Fernando, A. Quantum Communication for Video Transmission Over Error-Prone Channels. *IEEE Trans. Consum. Electron.* **2025**, *71*, 1148–1155. [CrossRef]
25. Sudhakar, K.; Tejnithish, S.; Thirupukal, G.; Arsath Farves, T.S. Next-Generation Wireless Networks: Advancements in Hybrid Beamforming for Massive MIMO Systems. In Proceedings of the 2025 International Conference on Advanced Computing Technologies (ICoACT), Sivalasi, India, 14–15 March 2025; pp. 1–7. [CrossRef]

26. Gaspar, D.; Mendes, L.L.; Pimenta, T.C. A Review on Principles, Performance and Complexity of Linear Estimation and Detection Techniques for MIMO Systems. *Front. Commun. Netw.* **2023**, *4*, 968370. [CrossRef]
27. Png, L.C.; Xiao, L.; Yeo, K.S.; Wong, T.S.; Guan, Y.L. MIMO-diversity switching techniques for digital transmission in visible light communication. In Proceedings of the 2013 IEEE Symposium on Computers and Communications (ISCC), Split, Croatia, 7–10 July 2013; pp. 576–582. [CrossRef]
28. Sachan, V.K.; Gupta, A.; Kumar, A. Performance analysis of MIMO space diversity technique for wireless communications. In Proceedings of the 2008 Fourth International Conference on Wireless Communication and Sensor Networks, Indore, India, 27–29 December 2008; pp. 153–156. [CrossRef]
29. Wang, Y.; Xiao, Y.; Xiao, M.; Li, N. Design of Dynamic Offset Spatial Modulation MIMO for Low-Cost Consumer Electronics Devices. *IEEE Trans. Consum. Electron.* **2024**, *70*, 7526–7534. [CrossRef]
30. Shanmuga Raja, K.; Jothi Lakshmi, G.R. Elevating Spectral Efficiency through Quantum-Inspired Deep Learning in Massive MIMO for 5G Communications. In Proceedings of the 2024 International Conference on Intelligent Systems for Cybersecurity (ISCS), Gurugram, India, 3–4 May 2024; pp. 1–5. [CrossRef]
31. Zhang, X.; Luo, Z.; Xiao, W.; Feng, L. Deep Learning-Based Modulation Recognition for MIMO Systems: Fundamental, Methods, Challenges. *IEEE Access* **2024**, *12*, 112558–112575. [CrossRef]
32. Feng, R.; Wang, C.X.; Huang, J.; Gao, X.; Salous, S.; Haas, H. Classification and Comparison of Massive MIMO Propagation Channel Models. *IEEE Internet Things J.* **2022**, *9*, 23452–23471. [CrossRef]
33. Urgelles, H.; Garcia-Roger, D.; Monserrat, J. Quantum-Based Maximum Likelihood Detection in MIMO-NOMA Systems for 6G Networks. *Quantum Rep.* **2024**, *6*, 533–549. [CrossRef]
34. Sayeed, A.M. Quantum MIMO: A Framework for Entanglement Distribution in Spatial Multipath Channels. In Proceedings of the Quantum 2.0 Conference and Exhibition, Washington, DC, USA, 13–16 June 2022. [CrossRef]
35. Shi, R.; Shi, J.; Guo, Y.; Peng, X.; Lee, M.H. Quantum MIMO Communication Scheme Based on Quantum Teleportation with Triplet States. *Int. J. Theor. Phys.* **2011**, *50*, 2334–2346. [CrossRef]
36. Kundu, N.K.; McKay, M.R.; Conti, A.; Mallik, R.K.; Win, M.Z. MIMO Terahertz Quantum Key Distribution Under Restricted Eavesdropping. *IEEE Trans. Quantum Eng.* **2023**, *4*, 4100315. [CrossRef]
37. Mikki, S. A Quantum MIMO Architecture for Antenna Wireless Digital Communications. *Prog. Electromagn. Res. C* **2019**, *93*, 143–156. [CrossRef]
38. ur Rehman, J.; Oleynik, L.; Koudia, S.; Bayraktar, M.; Chatzinotas, S. Diversity and Multiplexing in Quantum MIMO Channels. *EPJ Quantum Technol.* **2025**, *12*, 18. [CrossRef]
39. Kundu, N.K.; Dash, S.P.; McKay, M.R.; Mallik, R.K. MIMO Terahertz Quantum Key Distribution. *IEEE Commun. Lett.* **2021**, *25*, 3345–3349. [CrossRef]
40. Zhang, M.; Pirandola, S.; Delfanazari, K. Millimeter-Waves to Terahertz SISO and MIMO Continuous Variable Quantum Key Distribution. *IEEE Trans. Quantum Eng.* **2023**, *4*, 4100410. [CrossRef]
41. ur Rehman, J.; Rizvi, S.M.A.; Koudia, S.; Chatzinotas, S.; Shin, H. MIMO Quantum Communication in Correlated Pure-Loss Channels. *IEEE Commun. Lett.* **2025**, *29*, 1544–1548. [CrossRef]
42. Bross, B.; Chen, J.; Ohm, J.R.; Sullivan, G.J.; Wang, Y.K. Developments in international video coding standardization after AVC, with an overview of versatile video coding (VVC). *Proc. IEEE* **2021**, *109*, 1463–1493. [CrossRef]
43. Wieckowski, A.; da Silva, A.B.F.; Chaves, C.C.R.G.; Mendes, D.E.T.R. VVenC: An Open and Optimized VVC Encoder Implementation. In Proceedings of the 2021 IEEE International Conference on Multimedia and Expo Workshops (ICMEW), Shenzhen, China, 5–9 July 2021; pp. 1–2. [CrossRef]
44. Pathak, P.; Bhatia, R. Performance analysis of Polar codes for next generation 5G technology. In Proceedings of the 2022 3rd International Conference for Emerging Technology (INCET), Belgaum, India, 27–29 May 2022; pp. 1–4. [CrossRef]
45. Shepherd, D.J. On the Role of Hadamard Gates in Quantum Circuits. *Quantum Inf. Process.* **2006**, *5*, 161–177. [CrossRef]
46. Luo, Z.; Zhang, W. The Simulation Models for Rayleigh Fading Channels. In Proceedings of the 2007 Second International Conference on Communications and Networking in China, Shanghai, China, 22–24 August 2007; pp. 1158–1163. [CrossRef]
47. Nielsen, M.A.; Chuang, I.L. *Quantum Computation and Quantum Information: 10th Anniversary Edition*; Cambridge University Press: Cambridge, UK, 2010.
48. Barnum, H.; Nielsen, M.A.; Schumacher, B. Information transmission through a noisy quantum channel. *Phys. Rev. A* **1998**, *57*, 4153–4175. [CrossRef]
49. Miroshnichenko, T. People Playing Soccer. Available online: https://www.pexels.com/video/people-playingsoccer-6077718/ (accessed on 25 May 2025).
50. Midtrack, P. People Enjoying the Day in a Beach. Available online: https://www.pexels.com/video/people-enjoying-theday-in-a-beach-3150419/ (accessed on 25 May 2025).
51. Cup of Couple. A Bowl of Avocados and Vegetables. Available online: https://www.pexels.com/video/a-bowl-of-avocadosand-vegetables-7656166/(accessed on 25 May 2025).

52. International Telecommunication Union (ITU). *Methodologies for the Subjective Assessment of the Quality of Television Pictures*; ITU-R Recommendation BT.500; International Telecommunication Union: Geneva, Switzerland, 2022.
53. Thakur, V.S.; Kumar, A.; Das, J.; Dev, K.; Magarini, M. Quantum Error Correction Codes in Consumer Technology: Modeling and Analysis. *IEEE Trans. Consum. Electron.* **2024**, *70*, 7102–7111. [CrossRef]